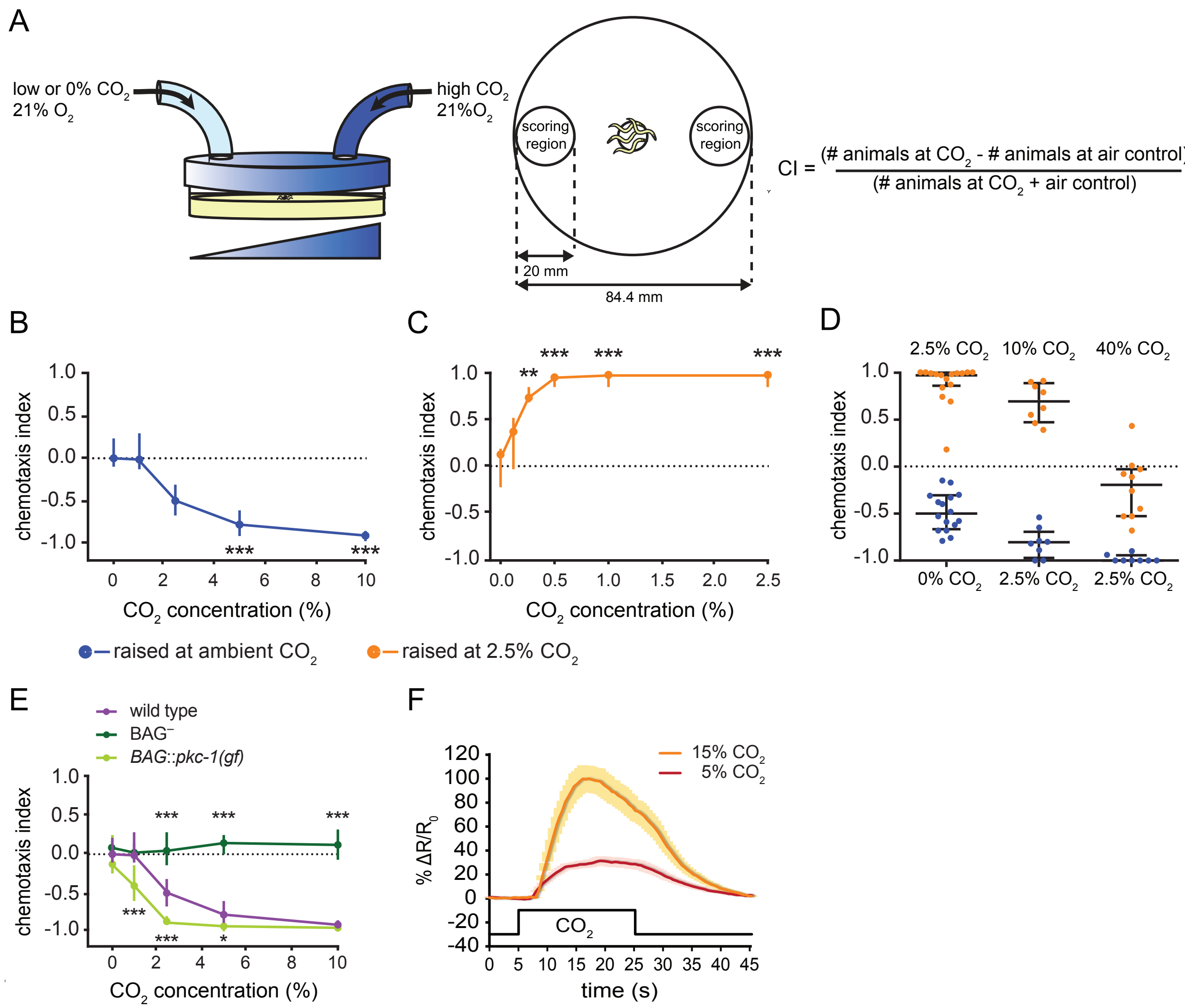

Figure S1. Related to Figure 1. CO_2 response in *C. elegans* is experience-dependent. (A) Schematic of the chemotaxis assay. Animals were placed in the center of a 100-mm agar plate (84.4-mm inside base diameter). A CO_2 gradient was established by delivering gas stimuli through holes on either side of the plate. At the end of the assay, the number of animals in a 20-mm diameter circle centered under each hole was counted and used to determine the chemotaxis index (CI) according to the formula shown above. (B-C) Animals raised at ambient CO_2 avoid CO_2 across concentrations (B), while animals raised at 2.5% CO_2 are attracted to CO_2 across concentrations (C). $^{**}p<0.01$, $^{***}p<0.001$, Kruskal-Wallis test with Dunn's post-test. For each graph, significance was determined relative to the 0% CO_2 condition. n=8-20 trials per condition. (D) Animals raised at either ambient or high (2.5%) CO_2 were tested in 0-2.5% (left), 2.5-10% (middle), or 2.5-40% (right) CO_2 gradients. Animals grown at ambient CO_2 migrate toward the lower CO_2 concentration. Animals grown at high CO_2 are attracted to the higher CO_2 concentration when tested in a 0-2.5% or 2.5-10% CO_2 gradient, but not when tested in a 2.5-40% CO_2 gradient. n=8-16 trials per condition. (E) BAG activity regulates behavioral sensitivity to CO_2. In animals raised at ambient CO_2, genetic ablation of the BAG neurons (BAG⁻) eliminates CO_2 avoidance across concentrations. By contrast, animals with more active BAG neurons due to BAG-specific expression of *pkc-1(gf)* show enhanced CO_2 avoidance. $^{*}p<0.05$, $^{***}p<0.001$, two-way ANOVA with Dunnett's post-test. n=8-16 trials per condition. For B-E, graphs depict medians with interquartile ranges. (F) The BAG response to CO_2 is concentration-dependent. Graph shows the calcium responses of BAG neurons to 15% CO_2 (orange) or 5% CO_2 (red), for animals raised at high (2.5%) CO_2, measured using the ratiometric calcium indicator yellow cameleon YC3.60. Solid lines indicate average calcium responses; shading represents SEM. Black line indicates the CO_2 pulse.

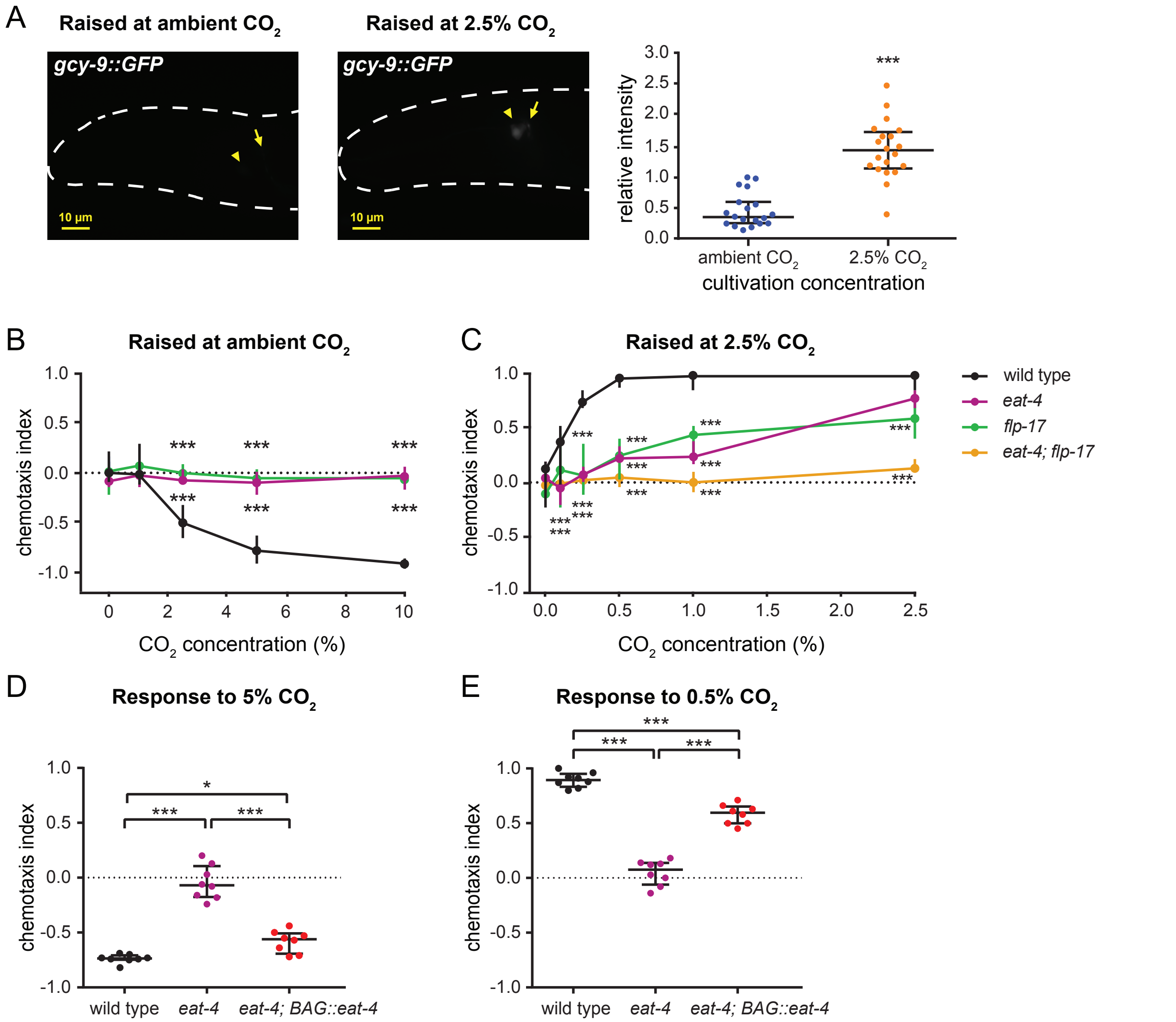

Figure S2. Related to Figure 1. BAG neurons mediate both attractive and aversive CO_2 responses. (A) Epifluorescence images of *gcy-9* expression in the BAG neurons of L4 animals raised at ambient CO_2 (left) or high (2.5%) CO_2 (middle). *gcy-9* expression was measured in animals containing a *gcy-9::GFP* transgene. Arrowheads indicate the location of the BAG neuron cell body; arrows indicate the location of the nerve ring. Anterior is to the left; dorsal is up. GFP expression is faint but detectable in animals raised at ambient CO_2, and brighter in animals raised at high CO_2. Graph (right) shows the relative intensity of expression of the *gcy-9::GFP* transgene in animals raised at ambient vs. high CO_2. ****p*<0.001, unpaired t test. n=19-20 animals per condition. (B-C) *eat-4* and *flp-17* are required for normal CO_2 response. (B) Mutation of *eat-4* or *flp-17* abolishes CO_2 avoidance in animals raised at ambient CO_2. ****p*<0.001, two-way ANOVA with Dunnett's post-test. n=6-16 trials per genotype and condition. (C) Mutation of either *eat-4* or *flp-17* reduces CO_2 attraction, and mutation of both genes abolishes CO_2 attraction, in animals raised at high (2.5%) CO_2. ****p*<0.001, two-way ANOVA with Dunnett's post-test. n=8-26 trials per genotype and condition. (D-E) *eat-4* acts in the BAG neurons to mediate CO_2 avoidance and CO_2 attraction. Restoring *eat-4* expression specifically in the BAG neurons of *eat-4* mutants partially restores CO_2 avoidance (D) and attraction (E). Animals were raised at ambient CO_2 (D) or 2.5% CO_2 (E) and tested for their response to 5% CO_2 or 0.5% CO_2, respectively. **p*<0.05, ****p*<0.001, one-way ANOVA with Sidak's post-test. n=8 trials per genotype and condition. For A-E, graphs show medians with interquartile ranges.

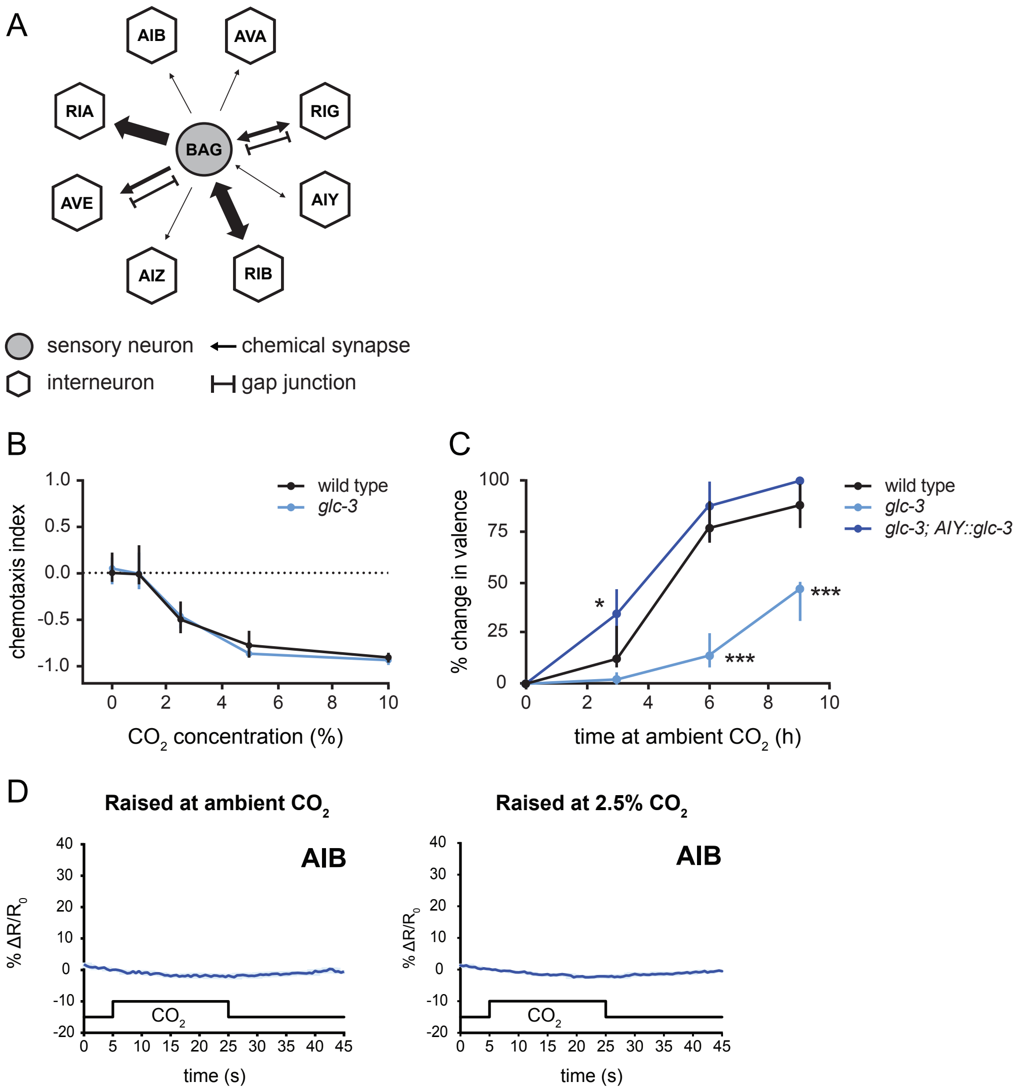

Figure S3. Related to Figure 2, Figure 3 and Figure 4. Distinct interneurons regulate CO_2 avoidance and attraction. (A) Structural connectivity of the CO_2-detecting BAG neurons. Arrow thickness reflects the number of synaptic connections (1-2 synapses, 4-7 synapses, or 10+ synapses) from BAG to the downstream interneurons [S1, S2]. The interneurons shown have documented functions in other chemosensory microcircuits and were therefore investigated in this study. The BAG sensory neurons are also presynaptic to several other interneurons not shown. (B) *glc-3* mutants show normal CO_2 avoidance when raised at ambient CO_2. (C) *glc-3* mutants show a delayed shift from CO_2 attraction to avoidance when raised at high (2.5%) CO_2 and transferred to ambient CO_2. Restoring *glc-3* function specifically to AIY (*AIY::glc-3*) rescues the shift in CO_2 response valence. Animals were tested for their response to 2.5% CO_2. Graph shows the percent change in valence as a function of time (see Methods). *$p<0.05$, ***$p<0.001$, two-way ANOVA with Sidak's post-test (B) or two-way ANOVA with Dunnett's post-test (C). n=8-24 trials per genotype and condition. For B-C, graphs show medians with interquartile ranges. (D) AIB is not activated by CO_2 in animals raised at ambient CO_2 or high (2.5%) CO_2. n=8 animals per genotype and condition. Calcium responses were measured using the ratiometric calcium indicators yellow cameleon YC3.60. Graphs show composite calcium responses to a 20-s pulse of 15% CO_2. Solid lines indicate average calcium responses; shading represents SEM.

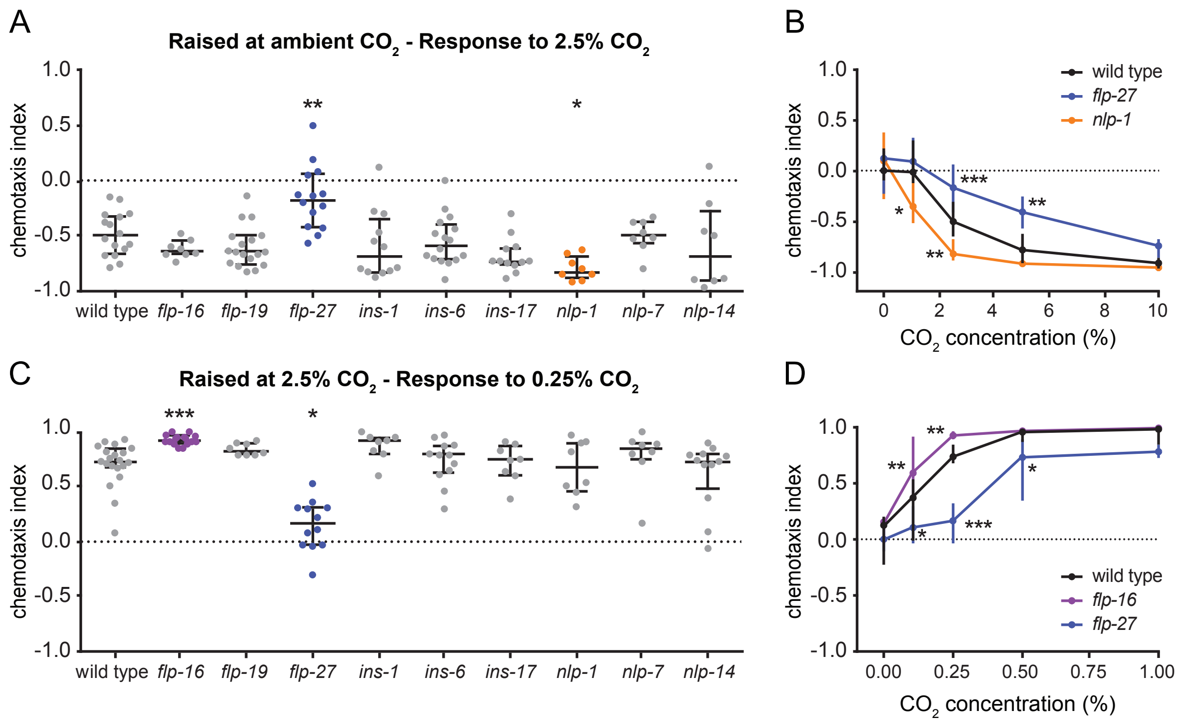

Figure S4. Related to Figure 4. A combinatorial code of neuropeptides regulates CO_2 response valence and sensitivity. (A-B) In animals raised at ambient CO_2, *flp-27* mutants show reduced CO_2 avoidance and *nlp-1* mutants show enhanced CO_2 avoidance. Graphs show responses to 2.5% CO_2 (A) or across CO_2 concentrations (B). *$p<0.05$, **$p<0.01$, ***$p<0.001$, one-way ANOVA with Dunnett's post-test (A) or two-way ANOVA with Dunnett's post-test (B). n=8-18 trials per genotype and condition. (C-D) In animals raised at high (2.5%) CO_2, *flp-16* mutants show enhanced CO_2 attraction and *flp-27* mutants show reduced attraction. Graphs show responses to 0.25% CO_2 (C) or across CO_2 concentrations (D). *$p<0.05$, **$p<0.01$, ***$p<0.001$, Kruskal-Wallis test with Dunn's post-test (C) or two-way ANOVA with Dunnett's post-test (D). n=6-20 trials per genotype and condition. For A-D, graphs show medians and interquartile ranges.

Supplemental References

S1. White, J.G., Southgate, E., Thomson, J.N., and Brenner, S. (1986). The structure of the nervous system of the nematode *Caenorhabditis elegans.* Philos. Trans. R. Soc. Lond. B. Biol. Sci. *314*, 1-340.

S2. Xu, M., Jarrell, T.A., Wang, Y., Cook, S.J., Hall, D.H., and Emmons, S.W. (2013). Computer assisted assembly of connectomes from electron micrographs: application to *Caenorhabditis elegans.* PLoS One *8*, 1-6.